

Lecture 14

Nonpremixed Turbulent Combustion: The Flamelet Concept

Models in nonpremixed turbulent combustion are often based on the presumed shape pdf approach.

This requires the knowledge of the Favre mean mixture fraction and its variance at position \mathbf{x} and time t .

A of the mixture fraction equation and using the gradient transport assumption led to the equation for the Favre mean mixture fraction

$$\bar{\rho} \frac{\partial \tilde{Z}}{\partial t} + \bar{\rho} \tilde{\mathbf{v}} \cdot \nabla \tilde{Z} = \nabla \cdot (\bar{\rho} D_t \nabla \tilde{Z})$$

Molecular diffusion is much smaller than the turbulent diffusion, and has therefore been neglected.

In addition to the mean mixture fraction we have derived an equation for the Favre variance of the mixture fraction

$$\bar{\rho} \frac{\partial \widetilde{Z''^2}}{\partial t} + \bar{\rho} \tilde{v} \cdot \nabla \widetilde{Z''^2} = -\nabla \cdot (\bar{\rho} \mathbf{v}'' \widetilde{Z''^2}) + 2\bar{\rho} D_t (\nabla \tilde{Z})^2 - \bar{\rho} \tilde{\chi}$$

where the gradient transport assumption

$$-\mathbf{v}'' \tilde{Z}'' = D_t \nabla \tilde{Z}_i$$

has again been used in the production term, second term of the r.h.s.

For the turbulent flux of the mixture fraction variance the gradient transport assumption

$$-\mathbf{v}'' \widetilde{Z''^2} = D_t \nabla \widetilde{Z''^2}$$

can also be used.

In

$$\bar{\rho} \frac{\partial \widetilde{Z''^2}}{\partial t} + \bar{\rho} \widetilde{v} \cdot \nabla \widetilde{Z''^2} = -\nabla \cdot (\bar{\rho} \widetilde{v'' Z''^2}) + 2\bar{\rho} D_t (\nabla \widetilde{Z})^2 - \bar{\rho} \widetilde{\chi}$$

the mean scalar dissipation rate appears, which as introduced in Lecture 10 will be modeled as

$$\widetilde{\chi} = c_\chi \frac{\widetilde{\varepsilon}}{\widetilde{k}} \widetilde{Z''^2}$$

where the time scale ratio c_χ is assumed to be a constant.

In the model

$$\tilde{\chi} = c_{\chi} \frac{\tilde{\varepsilon}}{\bar{k}} \widetilde{Z}''^2$$

Janicka and Peters (1982) found that a value of $c_{\chi}=2.0$ would predict the decay of scalar variance in an inert jet of methane very well.

Overholt and Pope (1996) and Juneja and Pope (1996) performing DNS studies of one and two passive scalar mixing find an increase of c_{χ} with Reynolds number and steady state values around 2.0 and 3.0, respectively.

In the numerical simulations of Diesel engine combustion, to be presented in Lecture 15, a value of $c_{\chi}=2.0$ has been used.

In many cases, as in turbulent jet diffusion flames in air, zero gradient boundary conditions, except at the inlet, can be imposed.

If the simplifying assumptions mentioned in Section 3.9 of Lecture 3 can be introduced the enthalpy h can be related to the mixture fraction by the linear coupling relation

$$h = h_2 + Z(h_1 - h_2)$$

which also holds for the mean values

$$\tilde{h} = h_2 + \tilde{Z}(h_1 - h_2)$$

and no additional equation for the enthalpy is required.

In $h = h_2 + Z(h_1 - h_2)$ and $\tilde{h} = h_2 + \tilde{Z}(h_1 - h_2)$

h_2 is the enthalpy of the air and h_1 that of the fuel.

A more general formulation is needed, if different boundary conditions have to be applied for the Favre mean mixture fraction and enthalpy or if heat loss due to radiation or unsteady pressure changes must be accounted for.

Then an equation for the Favre mean enthalpy as an additional variable must be solved.

This equation can be obtained from the enthalpy equation

$$\rho \frac{Dh}{Dt} = \rho c_p \frac{DT}{Dt} + \sum_{i=1}^k (-\mathbf{div} \mathbf{j}_i + \dot{m}_i) h_i.$$

by averaging

$$\bar{\rho} \frac{\partial \tilde{h}}{\partial t} + \bar{\rho} \tilde{\mathbf{v}} \cdot \nabla \tilde{h} = \frac{\partial \bar{p}}{\partial t} + \nabla \cdot (\bar{\rho} D_t \nabla \tilde{h}) + \bar{\dot{q}}_R$$

again a gradient transport equation for the correlation $-\tilde{\mathbf{v}}''\tilde{h}''$ has been introduced.

The term describing temporal mean pressure changes $\partial\bar{p}/\partial t$ has been retained, because it is important for the modeling of combustion in internal combustion engines operating under nonpremixed conditions, such as the Diesel engine.

The mean volumetric heat exchange term $\overline{\dot{q}_R}$ must also be retained in many applications where radiative heat exchange has an influence on the local enthalpy balance.

Changes of the mean enthalpy also occur due to convective heat transfer at the boundaries or due to the evaporation of a liquid fuel.

Temperature changes due to radiation within the flamelet structure also have a strong influence on the prediction of **NO_x formation** (cf. Pitsch et al. ,1998).

Presumed Shape Pdf Approach

The modelling equations can be used to calculate the mean mixture fraction and the mixture fraction variance at each point of the turbulent flow field, provided that the density field is known.

In addition, of course, equations for the turbulent flow field, the Reynolds stress equations (or the equation for the turbulent kinetic energy) and the equation for the dissipation must be solved.

In this approach a suitable two-parameter probability density function is "presumed" in advance, thereby fixing the functional form of the pdf by relating the two parameters in terms of the known values of the mean mixture fraction and its variance at each point of the flow field.

Since in a two-feed system the mixture fraction Z varies between $Z = 0$ and $Z = 1$, the [beta function pdf](#) is widely used for the Favre pdf in nonpremixed turbulent combustion.

The [beta-function pdf](#) has the form

$$\tilde{P}(Z; \mathbf{x}, t) = \frac{Z^{\alpha-1}(1-Z)^{\beta-1} \Gamma(\alpha + \beta)}{\Gamma(\alpha)\Gamma(\beta)}$$

Here Γ is the [gamma function](#).

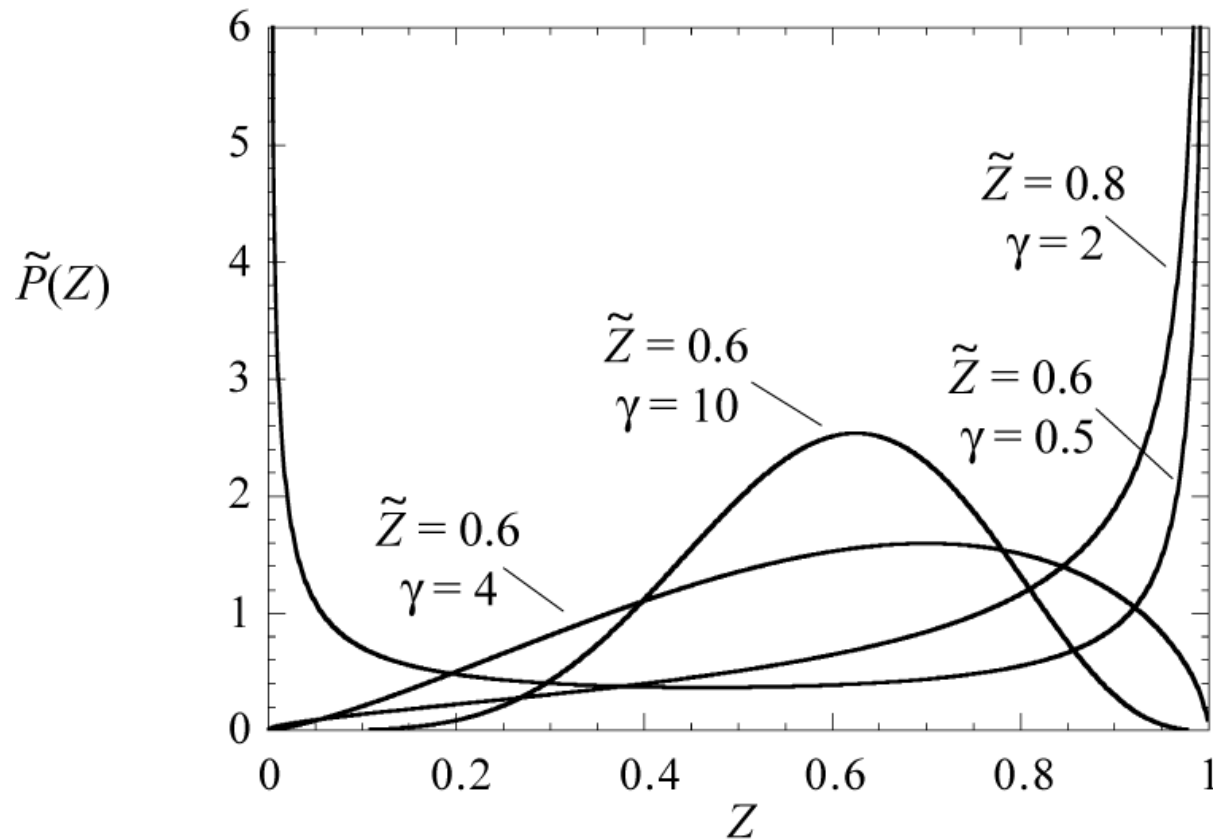
The two parameters α and β are related to the Favre mean mixture fraction and its variance by

$$\alpha = \tilde{Z}\gamma, \quad \beta = (1 - \tilde{Z})\gamma$$

where

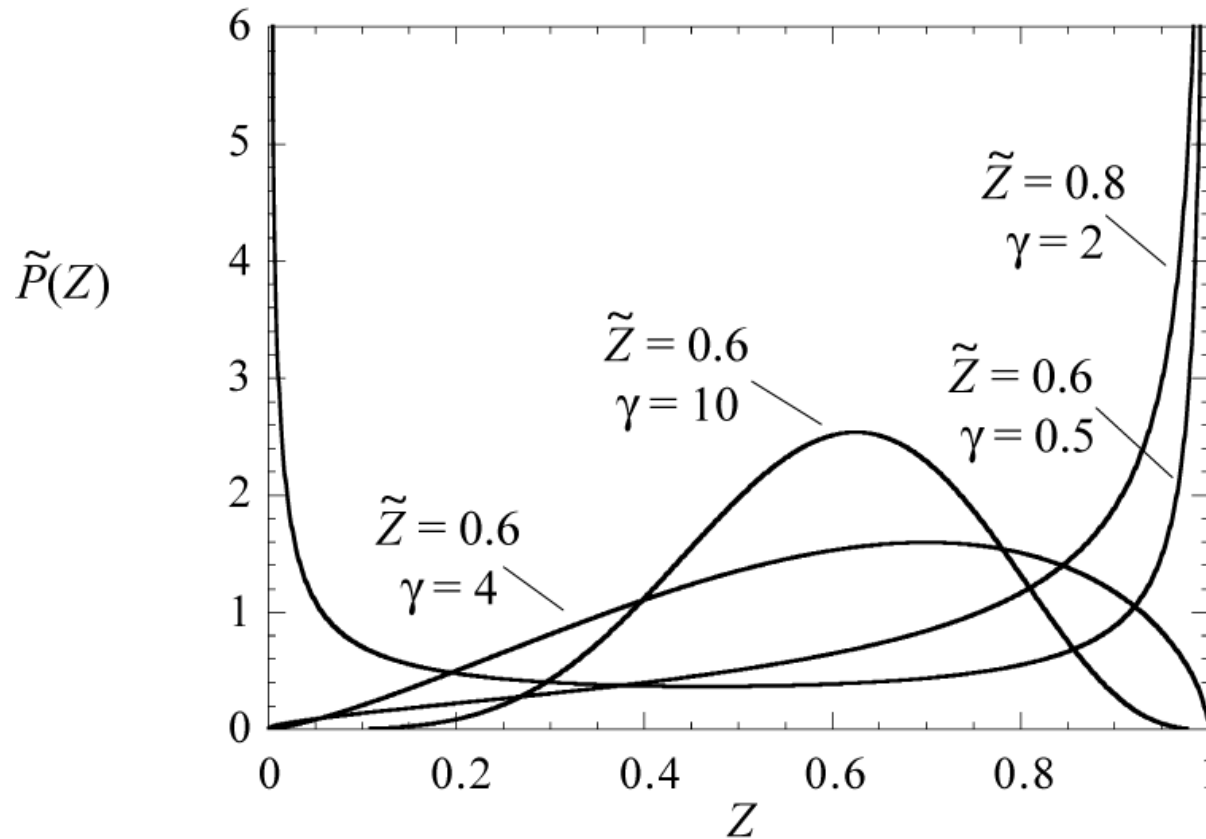
$$\gamma = \frac{\tilde{Z}(1 - \tilde{Z})}{\widetilde{Z'^2}} - 1 \geq 0$$

The beta-function plotted for different combinations of its parameters



It can be shown that in the limit of very small \tilde{Z}''^2 (large γ) it approaches a [Gaussian distribution](#).

For $\alpha < 1$ it develops a singularity at $Z = 0$ and for $\beta < 1$ a singularity at $Z = 1$.



Despite of its surprising flexibility, it is unable to describe distributions with a singularity at $Z = 0$ or $Z = 1$ and an additional intermediate maximum in the range $0 < Z < 1$.

By the presumed shape pdf approach means of any quantity that depends only on the mixture fraction can be calculated.

For instance, the mean value of ψ_i can be obtained from

$$\tilde{\psi}_i(\mathbf{x}, t) = \int_0^1 \psi_i(Z) \tilde{P}(Z; \mathbf{x}, t) dZ$$

A further quantity of interest is the mean density.

Since Favre averages are considered, one must take the Favre average of ρ^{-1} , which leads to

$$\widetilde{\rho^{-1}} = \frac{1}{\bar{\rho}} = \int_0^1 \rho^{-1}(Z) \tilde{P}(Z) dZ.$$

With

$$\tilde{P}(Z; \boldsymbol{x}, t) = \frac{Z^{\alpha-1}(1-Z)^{\beta-1} \Gamma(\alpha + \beta)}{\Gamma(\alpha)\Gamma(\beta)}, \quad \alpha = \tilde{Z}\gamma, \quad \beta = (1-\tilde{Z})\gamma$$
$$\gamma = \frac{\tilde{Z}(1-\tilde{Z})}{\tilde{Z}''^2} - 1 \geq 0$$

and the [Burke-Schumann solution](#) the [Conserved Scalar Equilibrium Model](#) for nonpremixed combustion is formulated.

It is based on a closed set of equations which do not require any further chemical input other than the assumption of [infinitely fast chemistry](#).

It may therefore be used as an initial guess in a calculation where the Burke-Schumann solution or the equilibrium solution later on is replaced by the solution of the [flamelet equations to account for non-equilibrium effects](#).

The Round Turbulent Jet Diffusion Flame

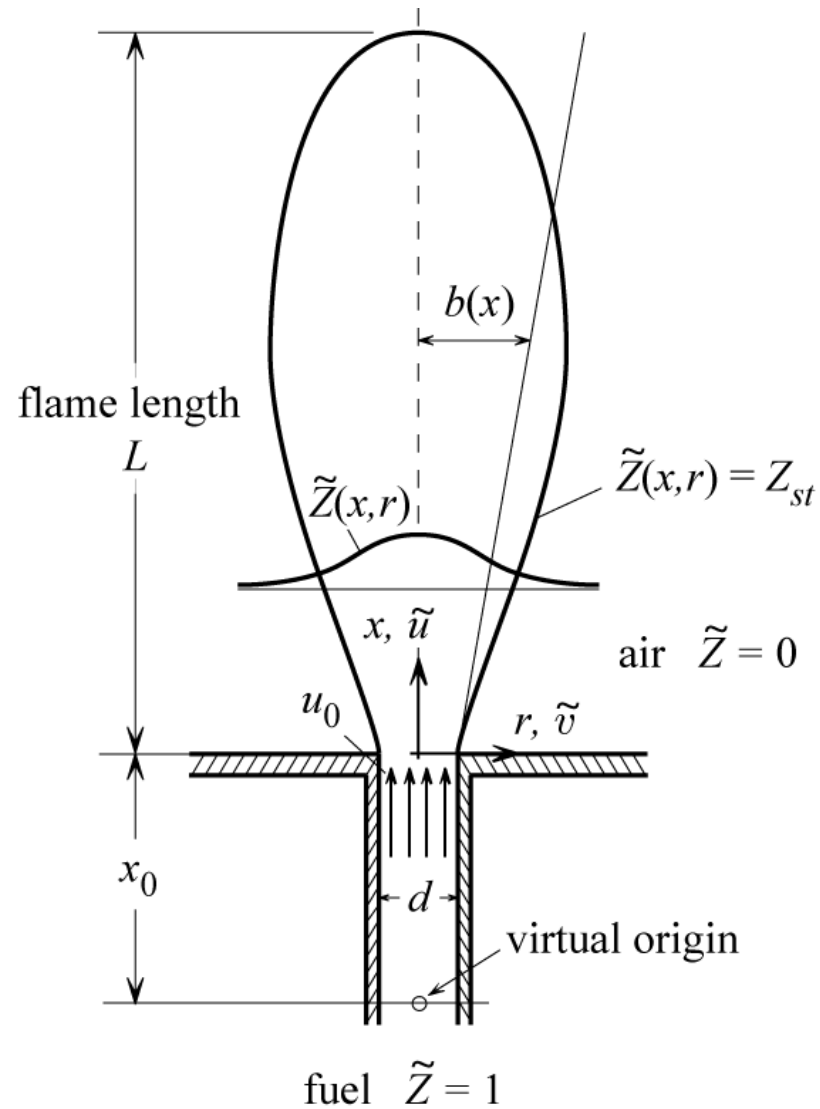
In many applications fuel enters into the combustion chamber as a turbulent jet, with or without swirl.

To provide an understanding of the basic properties of jet diffusion flames, we will consider here the easiest case, the [axisymmetric jet flame without buoyancy](#), for which we can obtain approximate analytical solutions.

This will enable us to determine, for instance, the flame length.

The flame length is defined as the distance from the nozzle to the point on the centerline of the flame where the mean mixture fraction is equal to Z_{st} .

The flow configuration for the round turbulent jet flame



Using Favre averaging and the the boundary layer assumption we obtain a system of two-dimensional axisymmetric equations

continuity

$$\frac{\partial}{\partial x} (\bar{\rho} \tilde{u} r) + \frac{\partial}{\partial r} (\bar{\rho} \tilde{v} r) = 0$$

momentum in x -direction

$$\bar{\rho} \tilde{u} r \frac{\partial \tilde{u}}{\partial x} + \bar{\rho} \tilde{v} r \frac{\partial \tilde{u}}{\partial r} = \frac{\partial}{\partial r} \left(\bar{\rho} \nu_t r \frac{\partial \tilde{u}}{\partial r} \right)$$

mean mixture fraction

$$\bar{\rho} \tilde{u} r \frac{\partial \tilde{Z}}{\partial x} + \bar{\rho} \tilde{v} r \frac{\partial \tilde{Z}}{\partial r} = \frac{\partial}{\partial r} \left(\frac{\bar{\rho} \nu_t r}{Sc_t} \frac{\partial \tilde{Z}}{\partial r} \right)$$

We have neglected molecular as compared to turbulent transport terms.

Turbulent transport was modeled by the gradient flux approximation.

For the scalar flux we have replaced D_t by introducing the turbulent Schmidt number $Sc_t = \nu_t / D_t$.

For simplicity, we will not consider equations for the turbulent kinetic energy and its dissipation or the mixture fraction variance but seek an approximate solution by introducing a model for the turbulent viscosity ν_t .

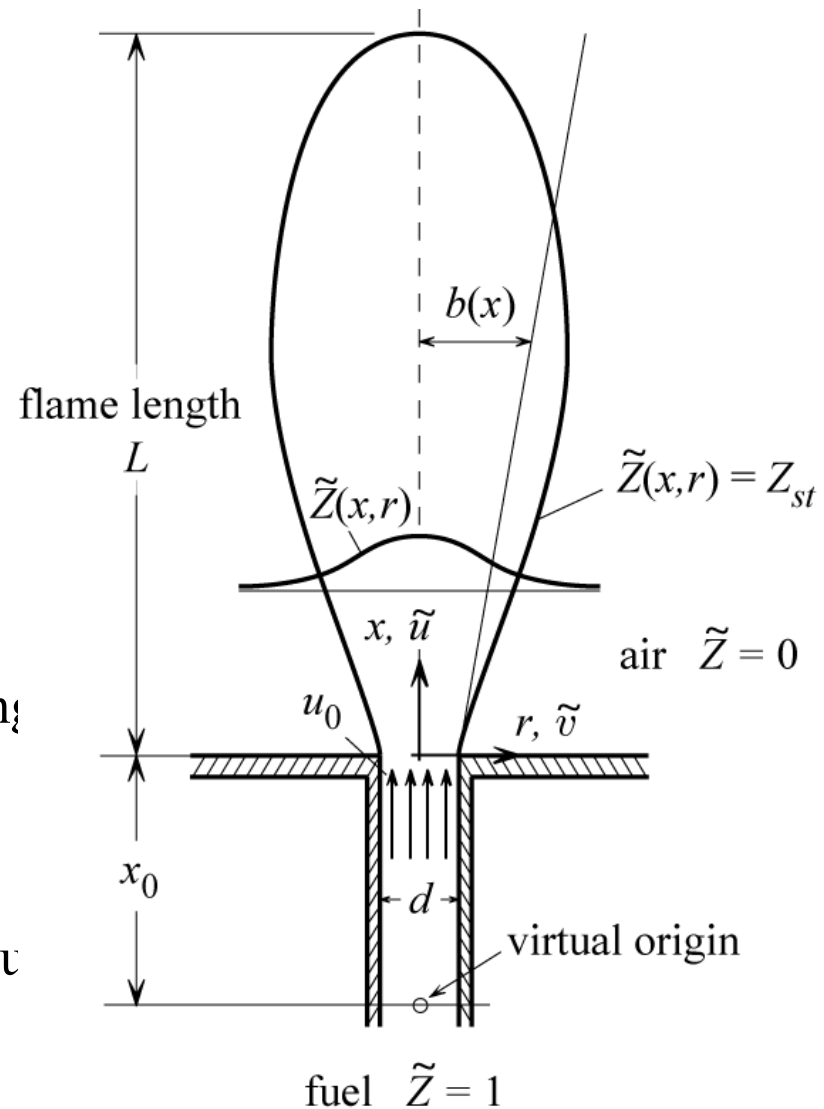
Details may be found in Peters and Donnerhack (1981).

As for the laminar solution of Lecture 9 for the round diffusion flame the dimensionality of the problem will again be reduced by introducing the similarity transformation

$$\eta = \frac{\bar{r}}{\xi}, \quad \bar{r}^2 = 2 \int_0^r \frac{\bar{\rho}}{\rho_\infty} r \, dr, \quad \xi = x + x_0,$$

which contains a density transformation defining co-ordinate.

The new axial co-ordinate ξ starts from the virtual origin located at $x = -x_0$.



Introducing a stream function ψ by

$$\bar{\rho}\tilde{u}r = \partial\psi/\partial r, \quad \bar{\rho}\tilde{v}r = -\partial\psi/\partial x$$

the continuity equation

$$\frac{\partial}{\partial x}(\bar{\rho}\tilde{u}r) + \frac{\partial}{\partial r}(\bar{\rho}\tilde{v}r) = 0$$

is satisfied.

In terms of the non-dimensional stream function $F(\eta)$ defined by

$$F(\eta) = \frac{\psi}{\rho_{\infty}\nu_{tr}\xi}$$

the axial and radial velocity components may now be expressed as

$$\tilde{u} = \frac{dF}{d\eta} \frac{\nu_{tr}}{\eta \xi}, \quad \bar{\rho}\tilde{v}r = -\rho_{\infty}\nu_{tr}\left(F - \frac{dF}{d\eta}\eta\right)$$

Here ν_{tr} is the eddy viscosity of a constant density jet, used as a reference value.

Differently from the laminar flame, where ν is a molecular property, ν_{tr} has been fitted (cf. Peters and Donnerhack (1981) to experimental data as

$$\nu_{tr} = \frac{u_0 d}{70}$$

For the mixture fraction the ansatz

$$\tilde{Z} = \tilde{Z}_{CL}(\xi) \tilde{\omega}(\eta)$$

is introduced, where \tilde{Z}_{CL} stands for the Favre mean mixture fraction on the centerline.

The system of equation for the turbulent round jet has the same similarity solution as the one derived in Section 9.2 of Lecture 9.

Here we approximate the Chapman-Rubesin parameter, however, as:

$$C = \frac{\bar{\rho}^2 \nu_t r^2}{\rho_\infty^2 \nu_{tr} \bar{r}^2}$$

In order to derive an analytical solution it must be assumed that C is a constant in the entire jet.

With a constant value of C and if the Schmidt number is replaced by a turbulent Schmidt number Sc_t one obtains the system of differential equations

$$-\frac{d}{d\eta}\left(\frac{F}{\eta}\frac{dF}{d\eta}\right) = \frac{d}{d\eta}\left(C\eta\frac{d}{d\eta}\left(\frac{1}{\eta}\frac{dF}{d\eta}\right)\right)$$

$$-\frac{d}{d\eta}(F\omega) = \frac{d}{d\eta}\left(\frac{C}{Sc_t}\eta\frac{d\omega}{d\eta}\right).$$

and its solution

$$F(\eta) = \frac{C(\gamma\eta)^2}{1 + (\gamma\eta/2)^2}, \quad \omega(\eta) = \left(\frac{1}{1 + (\gamma\eta/2)^2}\right)^{2Sc_t}$$

The solution reads

$$\tilde{u} = \frac{2C\gamma^2\nu_{tr}}{\xi} \left(\frac{1}{1 + (\gamma\eta/2)^2} \right)^2, \quad \tilde{\omega} = \left(\frac{1}{1 + (\gamma\eta/2)^2} \right)^{2Sc_t}$$

where the jet spreading parameter is now

$$\gamma^2 = \frac{3 \cdot 70^2}{64} \frac{\rho_0}{\rho_\infty C^2}$$

obtained from the requirement of integral momentum conservation along the axial direction.

Similarly, conservation of the mixture fraction integral across the jet yields the mixture fraction on the centerline

$$\tilde{Z}_{CL} = \frac{70(1 + 2 Sc_t)}{32} \frac{\rho_0 d}{\rho_\infty C \xi}$$

such that the mixture fraction profile is given by

$$\tilde{Z} = \frac{2.19(1 + 2 Sc_t) d}{x + x_0} \frac{\rho_0}{\rho_\infty C} \left(1 + \frac{1}{1 + (\gamma\eta/2)^2} \right)^{2 Sc_t}$$

From this equation the flame length L can be calculated by setting

$$\tilde{Z} = Z_{st} \quad \text{at} \quad x = L, r = 0$$

We get

$$\frac{L + x_0}{d} = \frac{2.19(1 + 2 Sc_t)}{Z_{st}} \frac{\rho_0}{\rho_\infty C}$$

Experimental data by Hawthorne et al. (1949) suggest that the flame length L should scale as

$$\frac{L + x_0}{d} = \frac{5.3}{Z_{st}} \left(\frac{\rho_0}{\rho_{st}} \right)^{1/2}$$

This fixes the turbulent Schmidt number as $Sc_t=0.71$ and the Chapman-Rubesin parameter as

$$C = \frac{(\rho_0 \rho_{st})^{1/2}}{\rho_\infty}$$

When this is introduced into the solution, one obtains the centerline velocity as

$$\frac{\tilde{u}_{CL}}{u_0} = \frac{6.56 d}{x + x_0} \left(\frac{\rho_0}{\rho_{st}} \right)^{1/2}$$

The distance of the virtual origin from $x = 0$ may be estimated by setting

$$\tilde{u}_{CL} = u_0 \quad \text{at} \quad x = 0$$

in

$$\frac{\tilde{u}_{CL}}{u_0} = \frac{6.56 d}{x + x_0} \left(\frac{\rho_0}{\rho_{st}} \right)^{1/2}$$

so that

$$x_0 = 6.56 d \left(\frac{\rho_0}{\rho_{st}} \right)^{1/2}$$

As an example for the flame length, we set the molecular weight at stoichiometric mixture equal to that of nitrogen, thereby estimating the density ratio ρ_0 / ρ_{st} from

$$\frac{\rho_0}{\rho_{st}} = \frac{W_0 T_{st}}{W_{N_2} T_0}$$

The flame length may then be calculated from

$$\frac{L + x_0}{d} = \frac{5.3}{Z_{st}} \left(\frac{\rho_0}{\rho_{st}} \right)^{1/2}$$

with $Z_{st} = 0.055$ as $L \sim 200 d$

In large turbulent diffusion flames buoyancy influences the turbulent flow field and thereby the flame length.

In order to derive a scaling law for that case, Peters and Görtgens (1991) have integrated the boundary layer equations for momentum and mixture fraction for a vertical jet flame over the radial direction in order to obtain first order differential equations in terms of the axial co-ordinate for cross-sectional averages of the axial velocity and the mixture fraction.

Since turbulent transport disappears entirely due to averaging, an empirical model for the entrainment coefficient β is needed, which relates the half-width b of the jet to the axial co-ordinate as

$$b(x) = \beta x$$

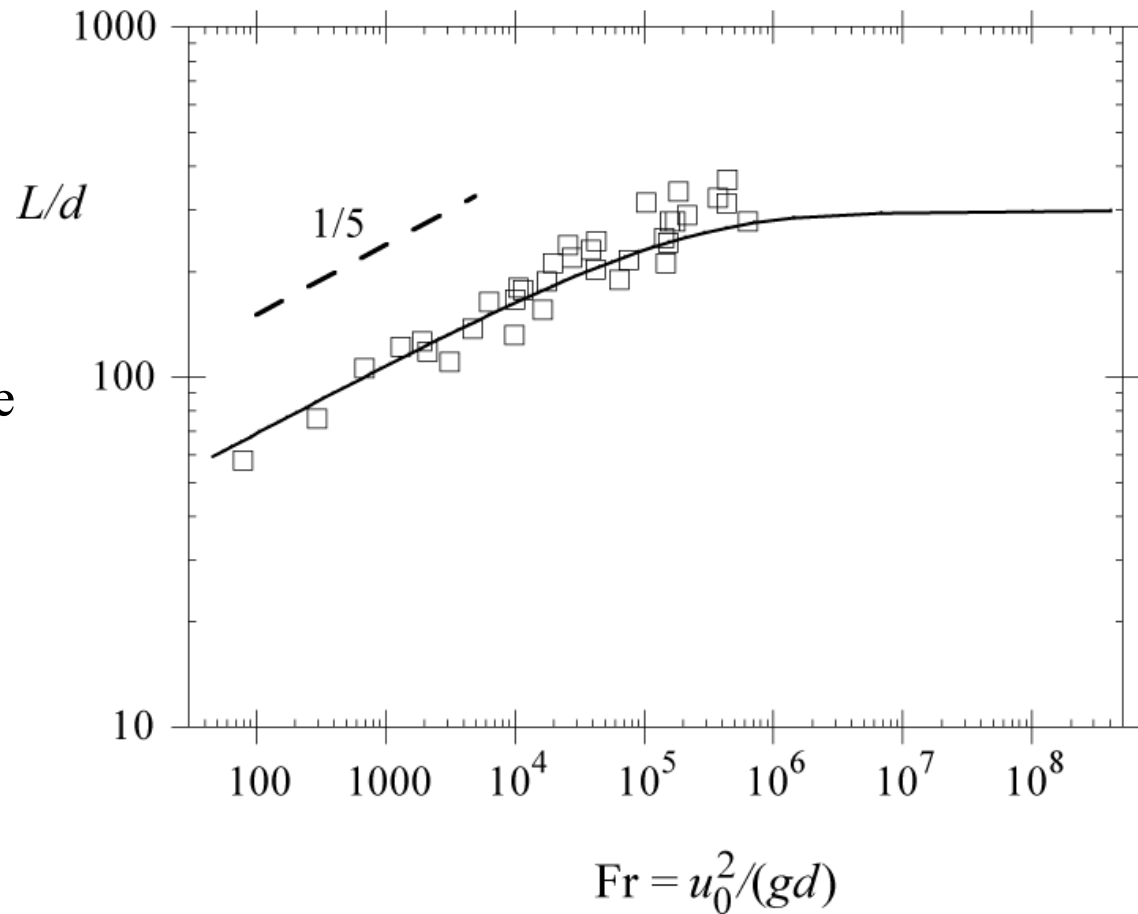
By comparison with the similarity solution for a non-buoyant jet β was determined as

$$\beta = 0.23 \left(\frac{\rho_{st}}{\rho_0} \right)^{1/2}$$

Details of the derivation may be found in Peters and Göttgens (1991).

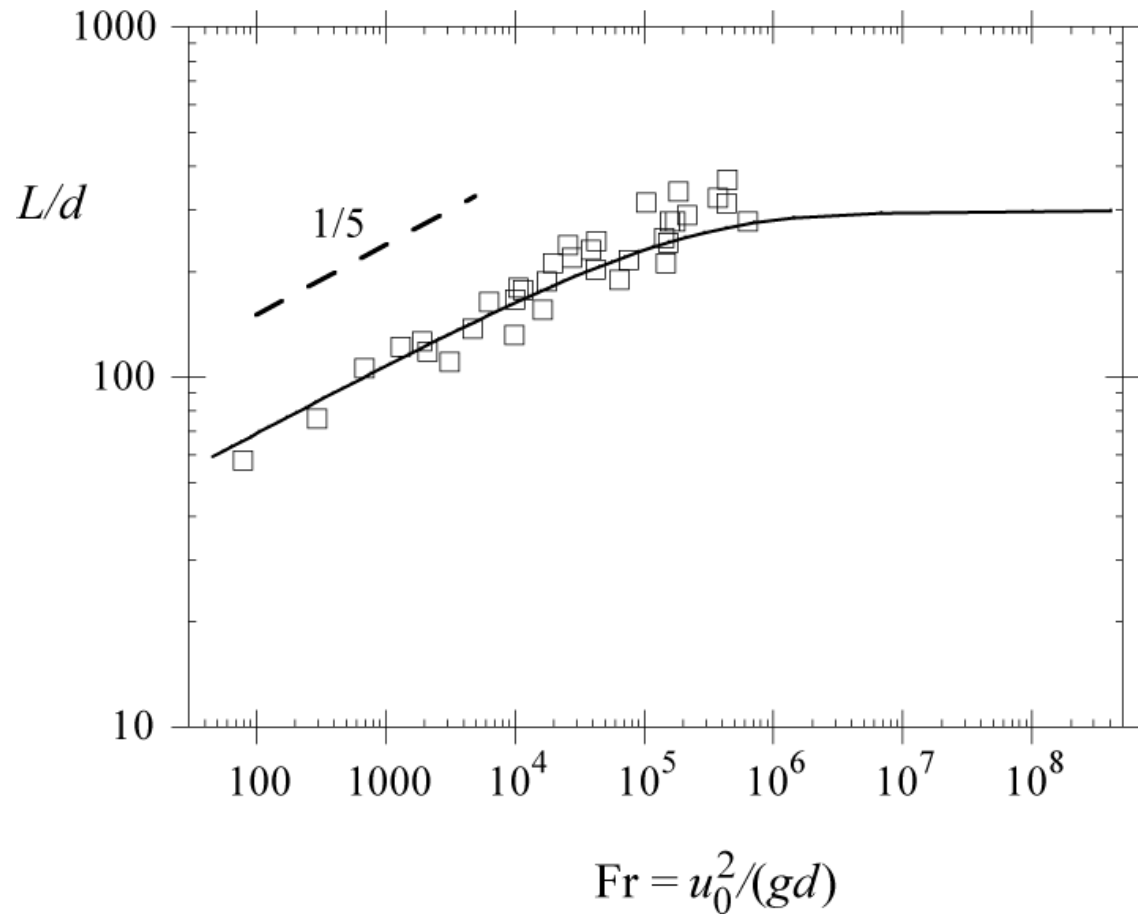
The predicted flame length of propane flames is compared with measurements from Sønju and Hustad (1984).

For Froude numbers smaller than 10^5 the data show a Froude number scaling as $Fr^{1/5}$, which corresponds to a balance of the second term on the l.h.s. with the term on the r.h.s.



For Froude numbers larger than 10^6 the flame length becomes Froude number independent equal to the value calculated from

$$\frac{L + x_0}{d} = \frac{5.3}{Z_{st}} \left(\frac{\rho_0}{\rho_{st}} \right)^{1/2}$$



Experimental Data from Turbulent Jet Diffusion Flames

There is a large body of experimental data on single point measurements using Laser Rayleigh and Raman scattering techniques combined with Laser-Induced Fluorescence (LIF).

Since a comprehensive review on the subject by Masri et al. (1996) is available, it suffices to present as an example the results by Barlow et al. (1990) obtained by the combined Raman-Rayleigh-LIF technique.

The fuel stream of the two flames that were investigated consisted of a mixture of 78 mole % H₂ and 22 mole % argon, the nozzle inner diameter d was 5.2 mm and the co-flow air velocity was 9.2 m/s.

The resulting flame length was approximately $L = 60 d$.

Two cases of exit velocities were analyzed, but only the case B with $u_0 = 150$ m/s will be considered here.

The stable species H_2 , O_2 , N_2 , and H_2O were measured using Raman-scattering at a single point with light from a flash-lamp pumped dye laser.

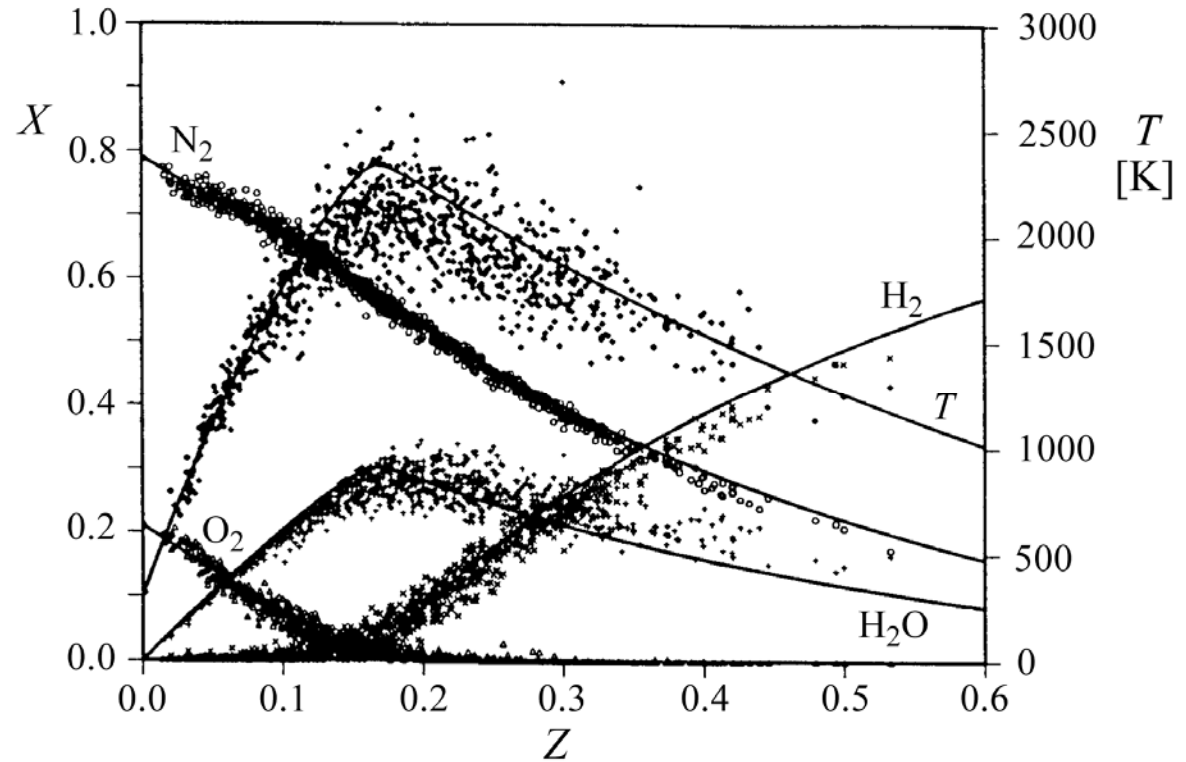
In addition, quantitative OH radical concentrations from LIF measurements were obtained by using the instantaneous one-point Raman data to calculate quenching corrections for each laser shot.

The temperature was calculated for each laser shot by adding number densities of the major species and using the perfect gas law.

An ensemble of one-point, one-time Raman-scattering measurements of major species and temperature plotted over mixture fraction are shown in the figure.

They were taken at $x/d = 30$, $r/d = 2$ in the case B flame.

Also shown are calculations based on the assumption of chemical equilibrium.

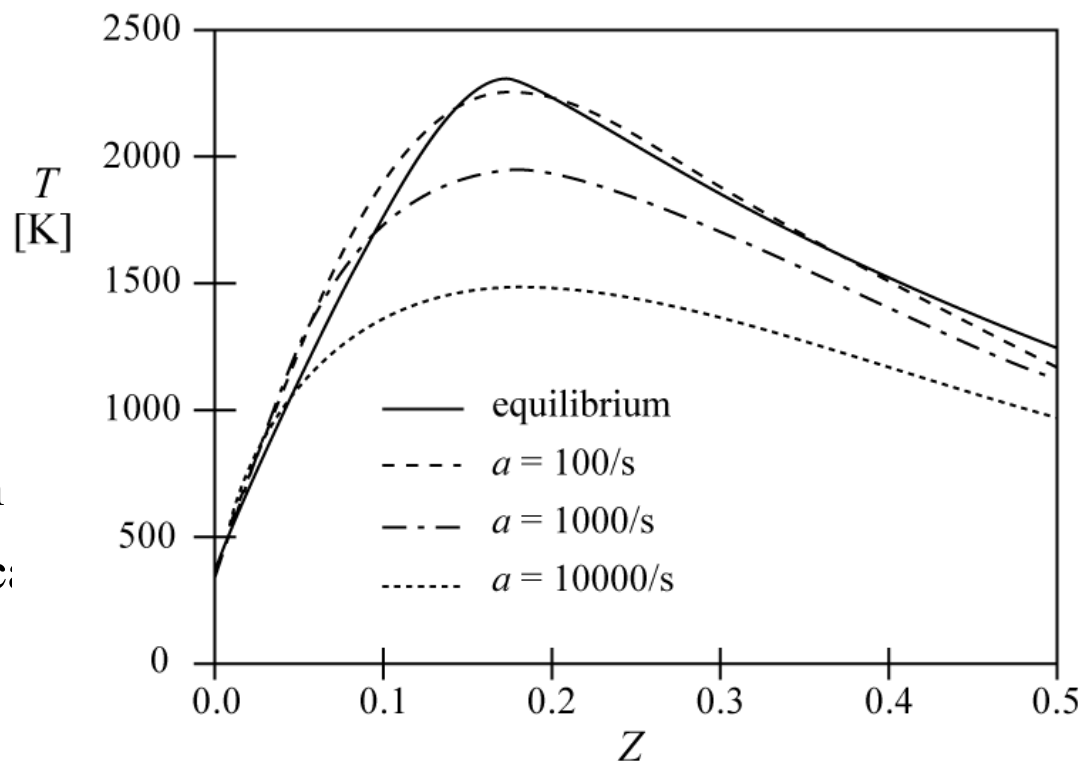


Temperature profiles versus mixture fraction calculated for counterflow diffusion flames at different strain rates

These steady state flamelet profiles display the characteristic decrease of the maximum temperature with increasing strain rates

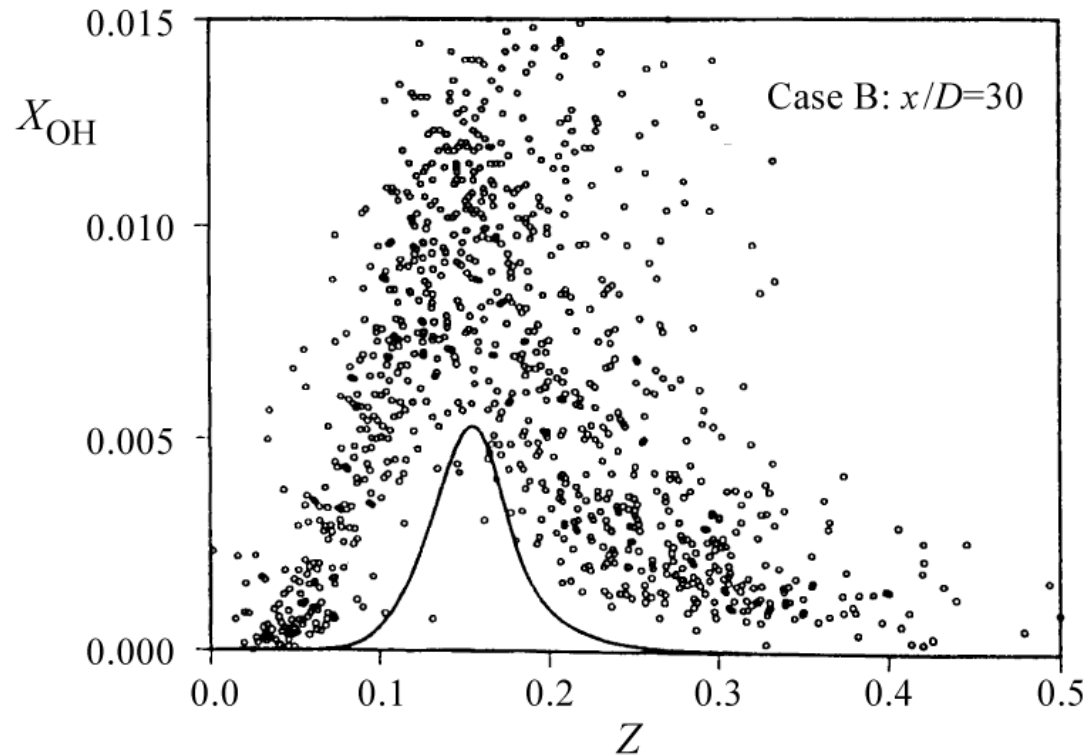
(which corresponds to decreasing Damköhler numbers) as shown schematically by the upper branch of the S-shaped curve.

The strain rates vary here between $a = 100/\text{s}$ which is close to chemical equilibrium and $a = 10000/\text{s}$.



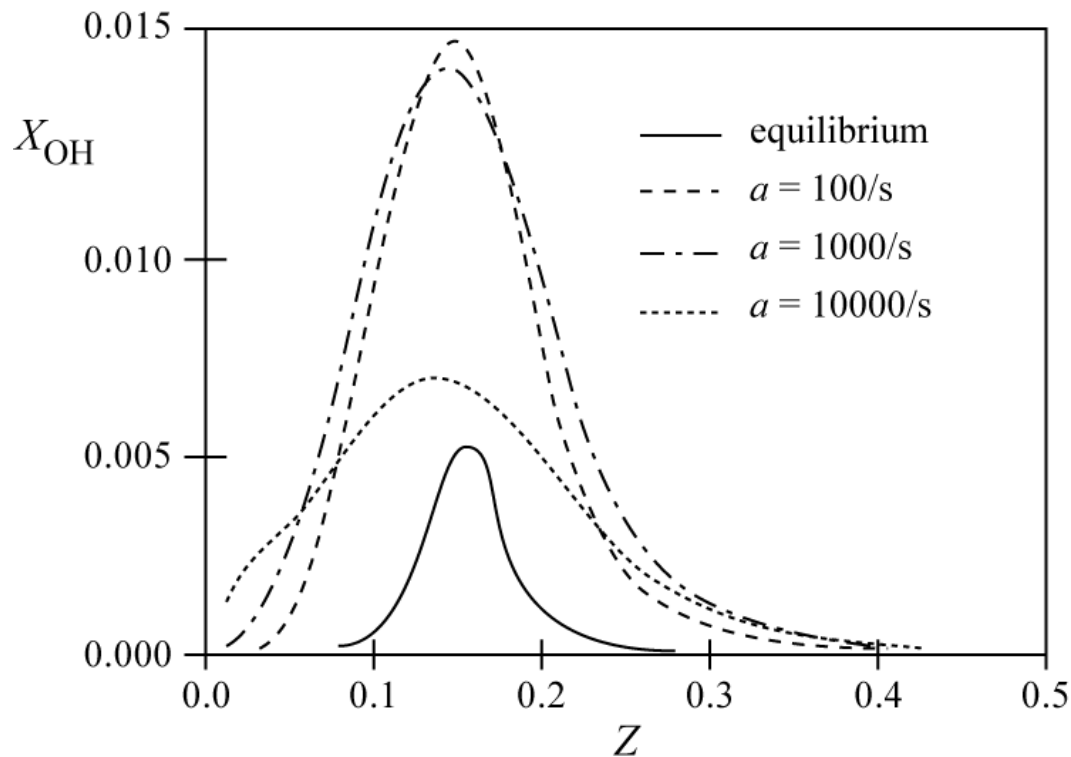
Data of OH-concentrations compared to flamelet calculations for the different strain rates mentioned before.

It is evident that the local OH-concentrations exceed those of the equilibrium profile by a factor up to 3.



The flamelet calculations show an increase of the maximum values by a factor of 3 already at the low strain rates $a = 100/\text{s}$ and $a = 1000/\text{s}$.

The maximum value of $a = 10000/\text{s}$ is close to extinction and does not represent conditions in the turbulent hydrogen flame considered here.



In summary, it may be concluded that one-point, one-time experimental data in turbulent flames, when plotted as a function of mixture fraction, show qualitatively similar tendencies as laminar flamelet profiles in counterflow diffusion flames.

Non-equilibrium effects are evident in both cases and lead to an increase of radical concentrations and a decrease of temperatures.

This has an important influence on NO_x formation in turbulent diffusion flames.

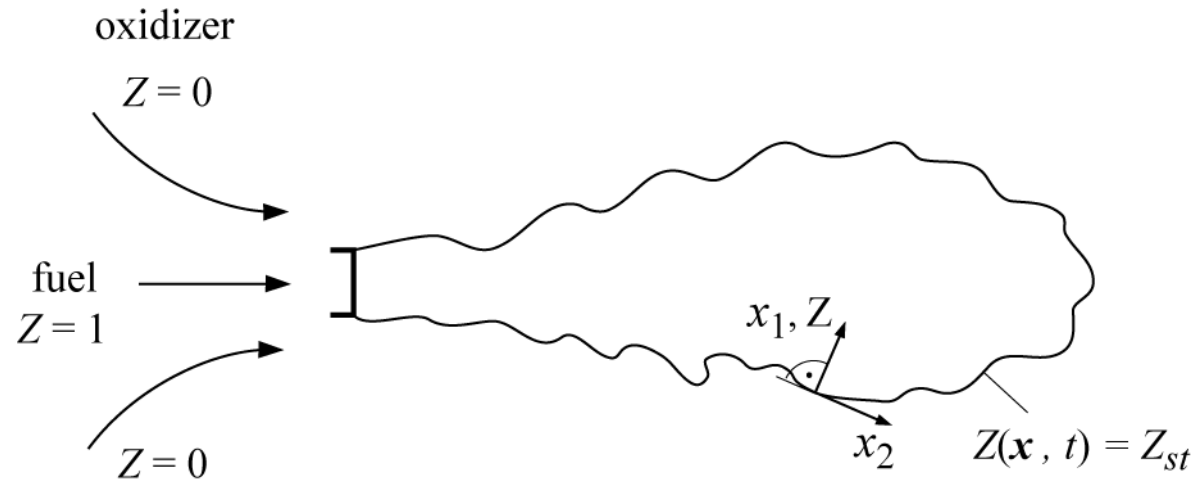
Laminar Flamelet Equations for Nonpremixed Combustion

Based on the laminar flamelet concept introduced in Lecture 8 the flame surface is defined as the surface of stoichiometric mixture which is obtained by setting

$$Z(\mathbf{x}, t) = Z_{st}$$

In the vicinity of that surface the reactive-diffusive structure can be described by the flamelet equations

$$\rho \frac{\partial \psi_i}{\partial t} = \frac{\rho}{Le_i} \frac{\partial^2 \psi_i}{\partial Z^2} + \omega_i$$



In these equations the [instantaneous scalar dissipation rate](#) has been introduced.

At the flame surface the instantaneous scalar dissipation rate takes the value χ_{st}

If χ is assumed to be a function of Z , this functional dependence can be parameterized by χ_{st} .

The scalar dissipation rate acts as an external parameter that is imposed on the flamelet structure by the mixture fraction field.

It has the dimension of an **inverse time** and therefore represents the **inverse of a diffusion time scale**.

It also can be thought of as a **diffusivity in mixture fraction space**.

In principle, both the mixture fraction Z and the scalar dissipation rate χ are **fluctuating quantities** and their statistical distribution needs to be considered, if one wants to calculate statistical moments of the reactive scalars (cf. Peters, (1984)).

If the joint pdf $\tilde{P}(Z, \chi_{st})$ surface, is known, and the steady state flamelet equations are solved to obtain ψ_i as a function of Z and χ_{st} , point \mathbf{x} and the time t .

The Favre mean of ψ_i can be obtained from

$$\tilde{\psi}_i(\mathbf{x}, t) = \int_0^1 \int_0^\infty \psi_i(Z, \chi_{st}) P(Z, \chi_{st}; \mathbf{x}, t) d\chi_{st} dZ$$

For further reading see Peters (1984).

If the unsteady term in the flamelet equation must be retained, joint statistics of Z and χ_{st} become impractical.

Then, in order to reduce the dimension of the statistics, it is useful to introduce **multiple flamelets**, each representing a different range of the χ -distribution.

Such multiple flamelets are used in the Eulerian Particle Flamelet Model (EPFM) by Barths et al. (1998).

Then the scalar dissipation rate can be formulated as a function of the mixture fraction.

Such a formulation can be used in modeling the conditional Favre mean scalar dissipation rate

$$\tilde{\chi}_Z = \frac{\langle \rho \chi | Z \rangle}{\langle \rho | Z \rangle}$$

Then the flamelet equations in a turbulent flow field take the form

$$\rho \frac{\partial \psi_i}{\partial t} = \frac{\rho}{\text{Le}_i} \frac{\tilde{\chi}_Z}{2} \frac{\partial \psi_i}{\partial Z} + \omega_i$$

A mean scalar dissipation rate, however, is unable to account for those ignition and extinction events that are triggered by small and large values of χ , respectively.

This is where **LES**, as discussed in Lecture 10, must be used.

With $\psi_i(Z, \tilde{\chi}_Z, t)$ obtained from solving

$$\rho \frac{\partial \psi_i}{\partial t} = \frac{\rho}{Le_i} \frac{\tilde{\chi}_Z}{2} \frac{\partial \psi_i}{\partial Z} + \omega_i$$

Favre mean values of ψ_i can be obtained at any point \mathbf{x} and time t in the flow

$$\tilde{\psi}_i(\mathbf{x}, t) = \int_0^1 \psi_i(Z, \tilde{\chi}_Z, t) \tilde{P}(Z; \mathbf{x}, t) dZ$$

Here the presumed shape of the pdf $\tilde{P}(Z; \mathbf{x}, t)$ can be calculated from the mean and the variance of the turbulent mixture fraction field, as discussed in Section 14.1.

Then there remains the problem on how to model the conditional scalar dissipation rate $\tilde{\chi}_Z$.

One then relates the conditional scalar dissipation rate $\tilde{\chi}_Z$ to that at a fixed value Z_{st} by

$$\tilde{\chi}_Z = \tilde{\chi}_{st} \frac{f(Z)}{f(Z_{st})}$$

where $f(Z)$ is a function as in

$$\chi \propto \exp(-2[\operatorname{erfc}^{-1}(2Z)]^2)$$

Then, with the presumed pdf $\tilde{P}(Z)$ being known, the unconditional average can be written as

$$\tilde{\chi} = \int_0^1 \tilde{\chi}_Z \tilde{P}(Z) dZ = \tilde{\chi}_{st} \int_0^1 \frac{f(Z)}{f(Z_{st})} \tilde{P}(Z) dZ$$

Therefore, using the model

$$\tilde{\chi} = c_\chi \frac{\tilde{\varepsilon}}{k} \tilde{Z}''^2$$

the conditional mean scalar dissipation rate $\tilde{\chi}_{st}$ can be expressed as

$$\tilde{\chi}_{st} = \frac{\tilde{\chi} f(Z_{st})}{\int_0^1 f(Z) \tilde{P}(Z) dZ}$$

which is to be used in $\tilde{\chi}_Z = \frac{\langle \rho \chi | Z \rangle}{\langle \rho | Z \rangle}$.

Flamelet equations can also be used to describe ignition in a nonpremixed system.

As the scalar dissipation rate decreases, as for instance in a Diesel engine after injection, heat release by chemical reactions will exceed heat loss out of the reaction zone, leading to auto-ignition.

The scalar dissipation rate at auto-ignition is denoted by

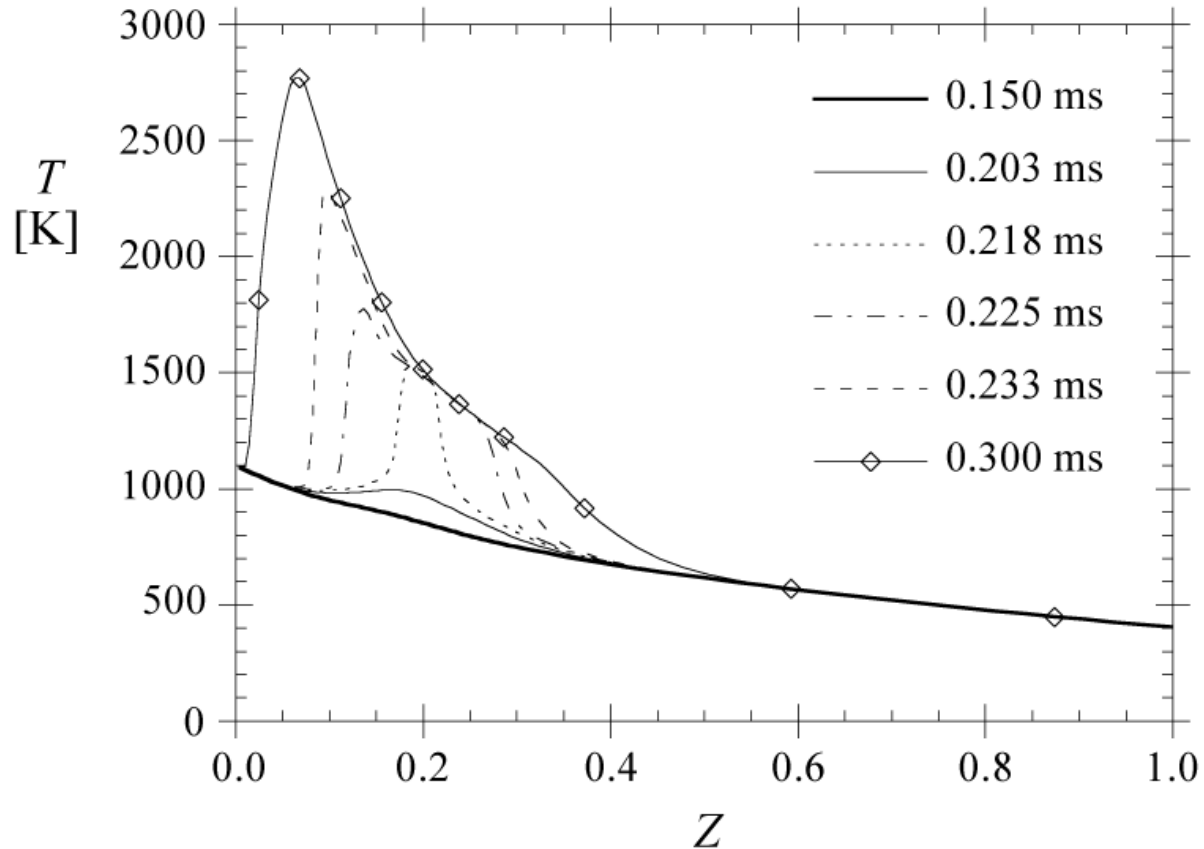
$$\chi_i = \chi_{st,ign}$$

For ignition under Diesel engine conditions this has been investigated by Pitsch and Peters (1998).

An example of auto-ignition of a *n*-heptane-air mixture calculated with the RIF code (cf. Paczko et al. (1999)) will be shown here.

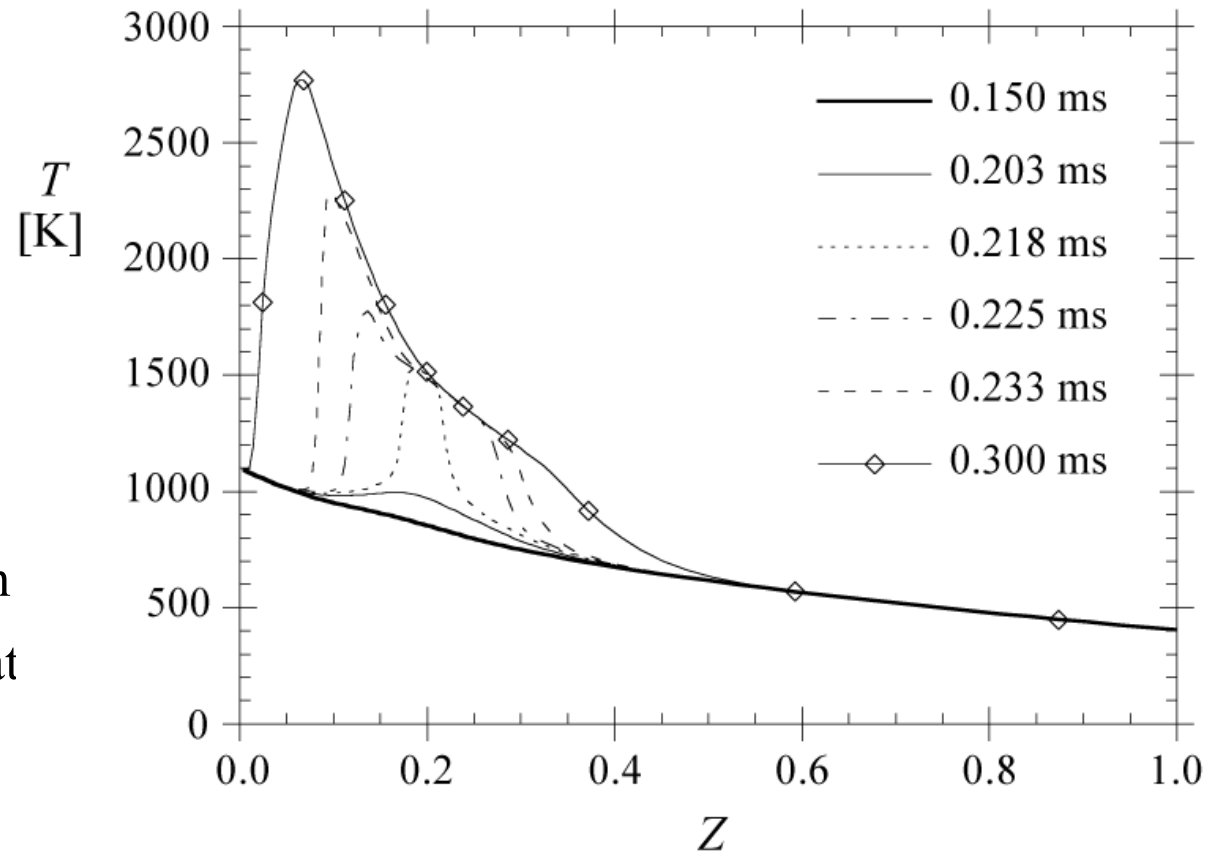
The initial air temperature is 1100 K and the initial fuel temperature is 400 K.

Mixing of fuel and air leads to a straight line for the enthalpy in mixture fraction space, but not for the temperature $T_u(Z)$, since the heat capacity c_p depends on temperature.



It is seen that auto-ignition starts after 0.203 ms, when the temperature profile shows already a small increase over a broad region around $Z=0.2$.

At $t=0.218$ ms there has been a fast thermal runaway in that region, with a peak at the adiabatic flame temperature.



Turbulent combustion models have also been used to predict NO_x formation in turbulent diffusion flames.

This is a problem of great practical importance, but due to the many physical aspects involved, it is also a very demanding test for any combustion model.

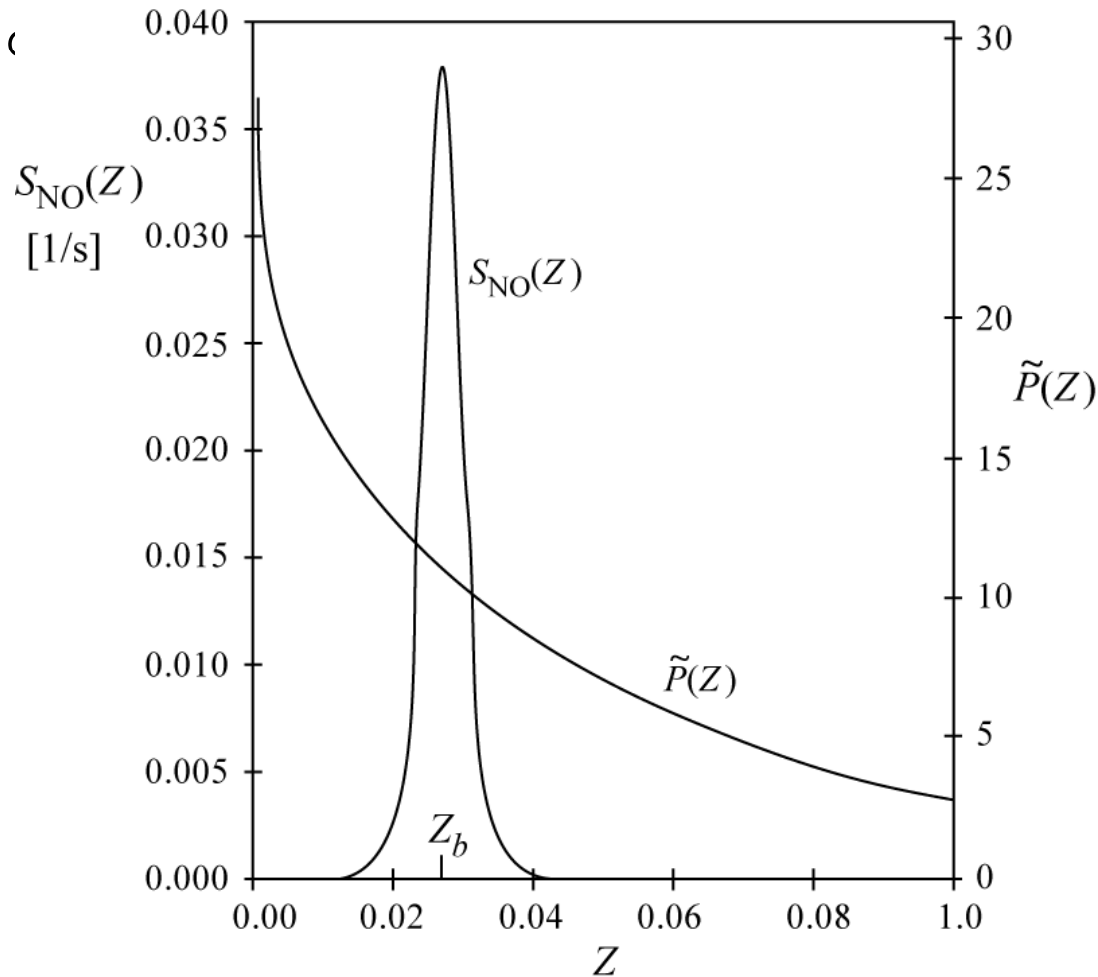
A very knowledgeable review on the various aspects of the problem has been given by Turns (1995).

A global scaling law for NO production in turbulent jet flames has been derived by Peters and Donnerhack (1981) assuming equilibrium combustion chemistry and thin NO reaction zone around the maximum temperature in mixture fraction space.

An asymptotic solution for the mean turbulent NO production rate can be obtained by realizing that in the expression

$$\bar{w}_{\text{NO}} = \bar{\rho} \tilde{S}_{\text{NO}} = \bar{\rho} \int_0^1 S_{\text{NO}}(Z) \tilde{P}(Z) dz$$

the function $S_{\text{NO}}(Z)$ has a very strong peak in the vicinity of the maximum temperature, but decreases very rapidly to both sides (shown for a hydrogen flame).



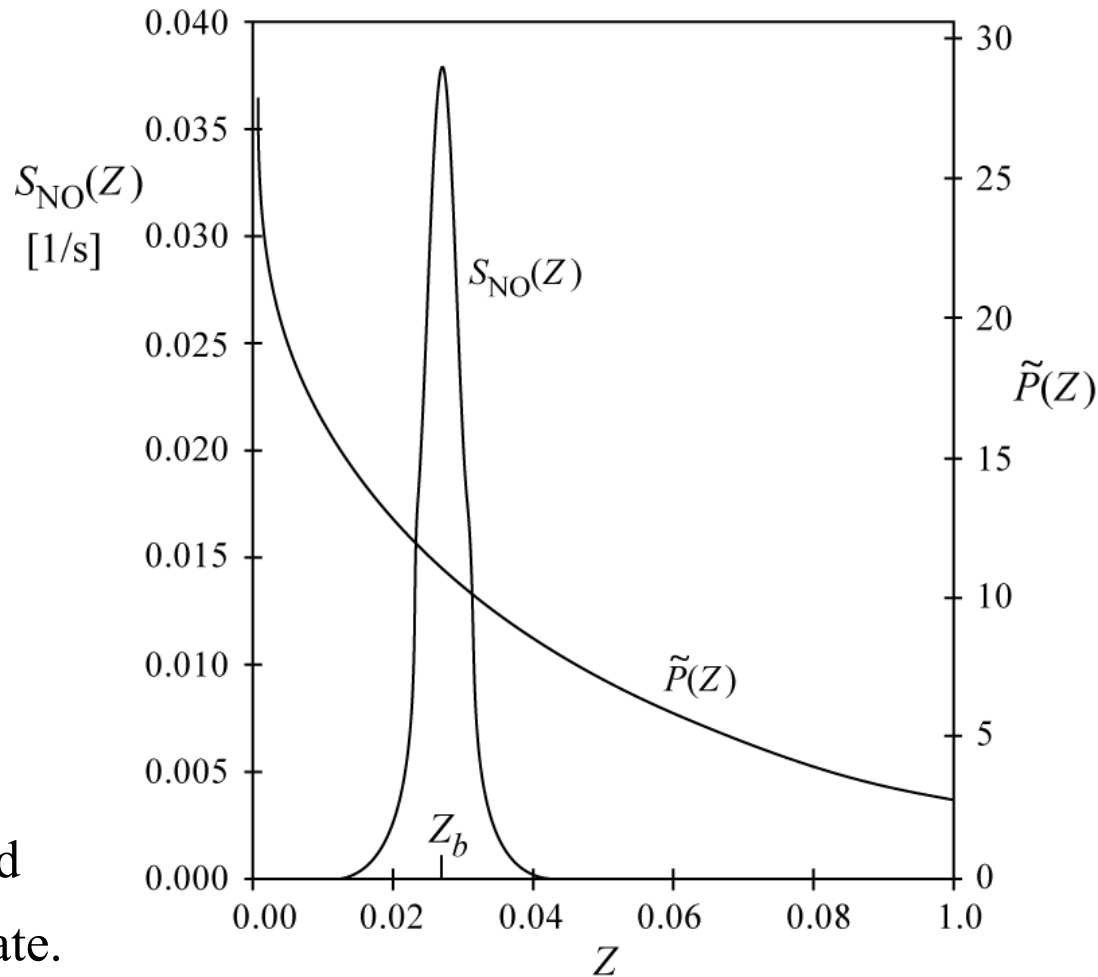
The NO reaction rate acts nearly like a δ -function underneath the integral in

$$\bar{\omega}_{\text{NO}} = \bar{\rho} \tilde{S}_{\text{NO}} = \bar{\rho} \int_0^1 S_{\text{NO}}(Z) \tilde{P}(Z) dZ$$

It has been shown by Peters (1978) and Janicka and Peters (1982) that an asymptotic expansion of the reaction rate around the maximum temperature leads to

$$\bar{\omega}_{\text{NO}} = \bar{\rho} \tilde{P}(Z_b) \varepsilon S_{\text{NO}}(Z_b)$$

where Z_b is the mixture fraction at the maximum temperature T_b and $S_{\text{NO}}(Z_b)$ is the maximum reaction rate.



The quantity ε represents the reaction zone thickness of NO production in mixture fraction space.

That quantity was derived from the asymptotic theory as

$$\varepsilon = \left(\frac{-2RT_b^2}{Z_b^2 E_{\text{NO}} (d^2T/dZ^2)_{T_b}} \right)^{1/2}$$

Here E_{NO} is the activation energy of the NO production rate.

Finally, Peters and Donnerhack (1981) predicted the NO emission index E_{NO} , which represents the total mass flow rate of NO produced per mass flow rate of fuel, as being proportional to

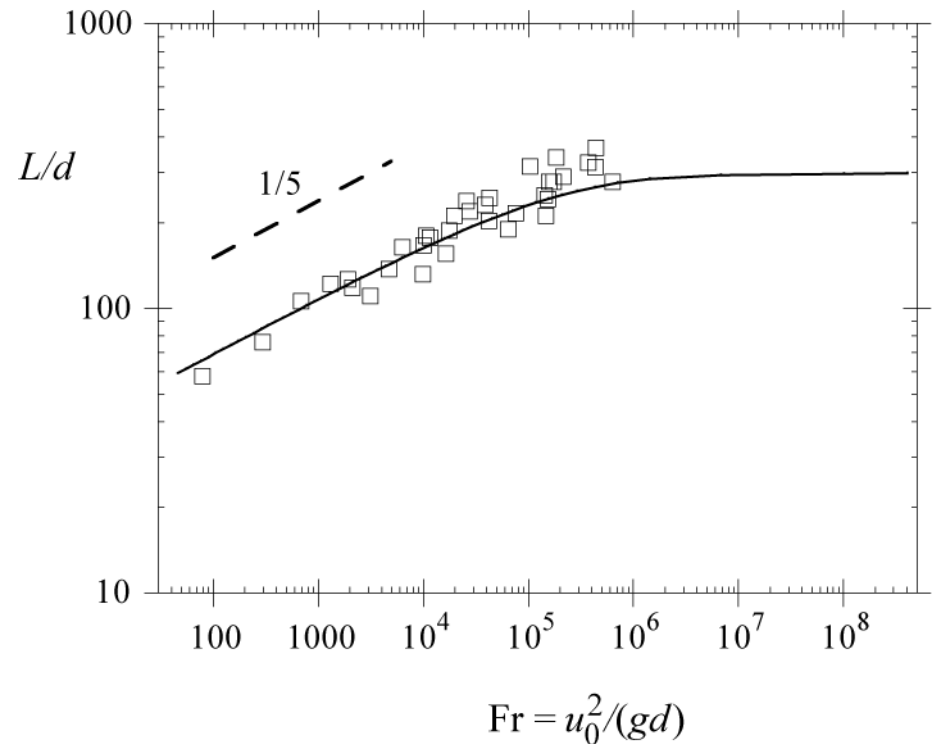
$$E_{\text{NO}} \sim S_{\text{NO}}(Z_b) \varepsilon \left(\frac{L}{d} \right)^3 \frac{d}{u_0}$$

In

$$\text{EINO} \sim S_{\text{NO}}(Z_b)\varepsilon \left(\frac{L}{d}\right)^3 \frac{d}{u_0}$$

L is the flame length, d the nozzle diameter and u_0 the jet exit velocity.

The normalized flame length L/d is constant for momentum dominated jets but scales with the Froude number $\text{Fr}=u_0^2/(gd)$ as $L/d \sim \text{Fr}^{1/5}$ for buoyancy dominated jets as shown in the figure.

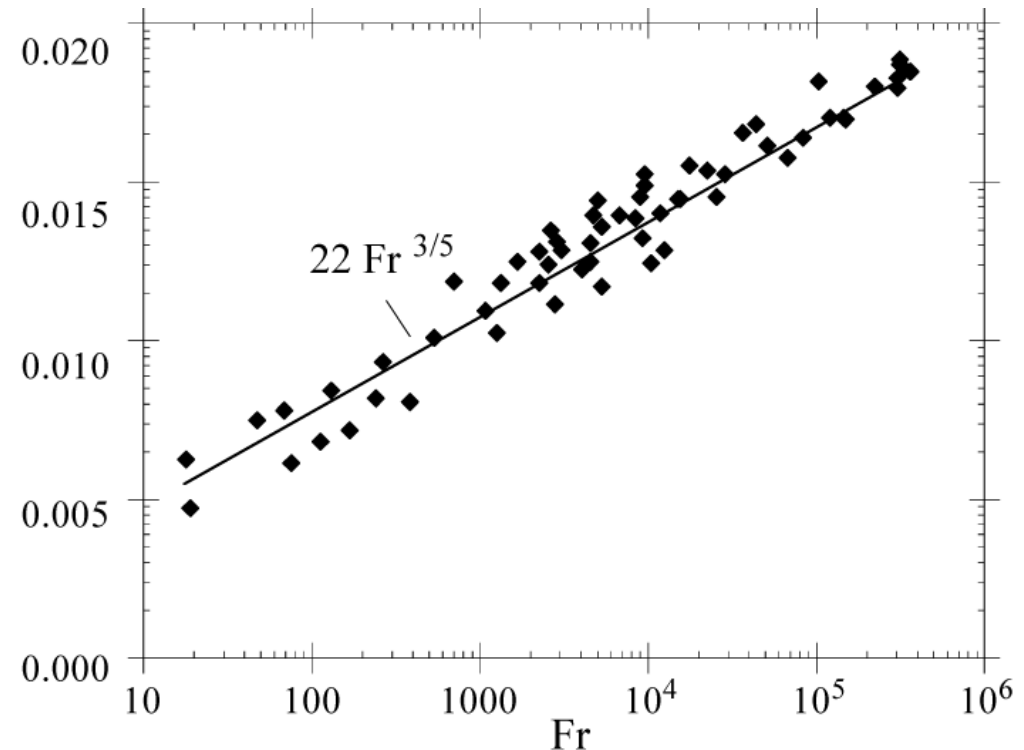


This explains, for instance, the $Fr^{3/5}$ dependence of the emission index found in the buoyancy dominated propane jet diffusion flames of Røkke et al. (1992).

These data are reproduced here together with the prediction of the NO_x emission index (expressed here in terms of NO_2)

$$\frac{EINO_x}{d/u_0} \left[\frac{gNO_2}{kg s} \right]$$

$$\frac{EINO_x}{d/u_0} = 22 Fr^{3/5} \left[\frac{gNO_2}{kg fuel s} \right]$$



An interesting set of experimental data are those by Chen and Driscoll (1990) and Driscoll et al. (1992) for diluted hydrogen flames.

These data show a square root dependence of the rescaled emission index on the Damköhler number.

An explanation for this scaling may be found by using the steady state flamelet equation for the second derivative of temperature in

$$\varepsilon = \left(\frac{-2RT_b^2}{Z_b^2 E_{\text{NO}} (d^2T/dZ^2)_{T_b}} \right)^{1/2}$$

rather than the equilibrium profile.

This may be written as

$$\frac{d^2T}{dZ^2} \sim \frac{\omega_T}{\chi}$$

Here the term on the r.h.s., evaluated at and divided by the maximum temperature, may also be interpreted as a Damköhler number.

Inserting this into

$$\varepsilon = \left(\frac{-2RT_b^2}{Z_b^2 E_{\text{NO}} (d^2T/dZ^2)_{T_b}} \right)^{1/2}$$

the quantity ε becomes proportional to $\text{Da}^{-1/2}$.

This finally leads with

$$\frac{EINO}{(L/d)^3} \sim \varepsilon Da$$

to

$$\frac{EINO}{(L/d)^3} \sim Da^{1/2}$$

This scaling law indicates that the experimentally observed $(d/u^0)^{1/2}$ dependence of the rescaled NO emission index is a **residence time effect**, modified by the temperature sensitivity of the NO reaction rate, on which the asymptotic theory by Peters and Donnerhack (1981) was built.

It also shows that unsteady effects of the flame structure and super-equilibrium O-concentrations may be of less importance than is generally assumed.

Appendix

As in

and

$$\bar{\rho} \frac{\partial \tilde{Z}}{\partial t} + \bar{\rho} \tilde{\mathbf{v}} \cdot \nabla \tilde{Z} = \nabla \cdot (\bar{\rho} D_t \nabla \tilde{Z})$$

the transport term

$$\bar{\rho} \frac{\partial \tilde{Z}''^2}{\partial t} + \bar{\rho} \tilde{\mathbf{v}} \cdot \nabla \tilde{Z}''^2 = -\nabla \cdot (\bar{\rho} \mathbf{v}'' \tilde{Z}''^2) + 2\bar{\rho} D_t (\nabla \tilde{Z})^2 - \bar{\rho} \tilde{\chi}''^2$$

ected

as being small compare

$$\bar{\rho} \frac{\partial \tilde{h}}{\partial t} + \bar{\rho} \tilde{\mathbf{v}} \cdot \nabla \tilde{h} = \frac{\partial \bar{p}}{\partial t} + \nabla \cdot (\bar{\rho} D_t \nabla \tilde{h}) + \bar{q}_R$$

Effects due to non-unity Lewis numbers have also been neglected.

No equation for enthalpy fluctuations is presented here, because in nonpremixed turbulent combustion, it is often assumed that fluctuations of the enthalpy are mainly due to mixture fraction fluctuations and are described by those.

If the assumption of fast chemistry is introduced and the coupling between the mixture fraction and the enthalpy

$$h = h_2 + Z(h_1 - h_2)$$

can be used, the [Burke-Schumann solution](#) or the equilibrium solution relates all reactive scalars to the local mixture fraction.

Using these relations the easiest way to obtain mean values of the reactive scalars is to use the [presumed shape pdf approach](#).

This is called the [Conserved Scalar Equilibrium Model](#).

For such shapes, which have been found in jets and shear layers, a composite model has been developed by Effelsberg and Peters (1983).

It identifies three different contributions to the pdf:

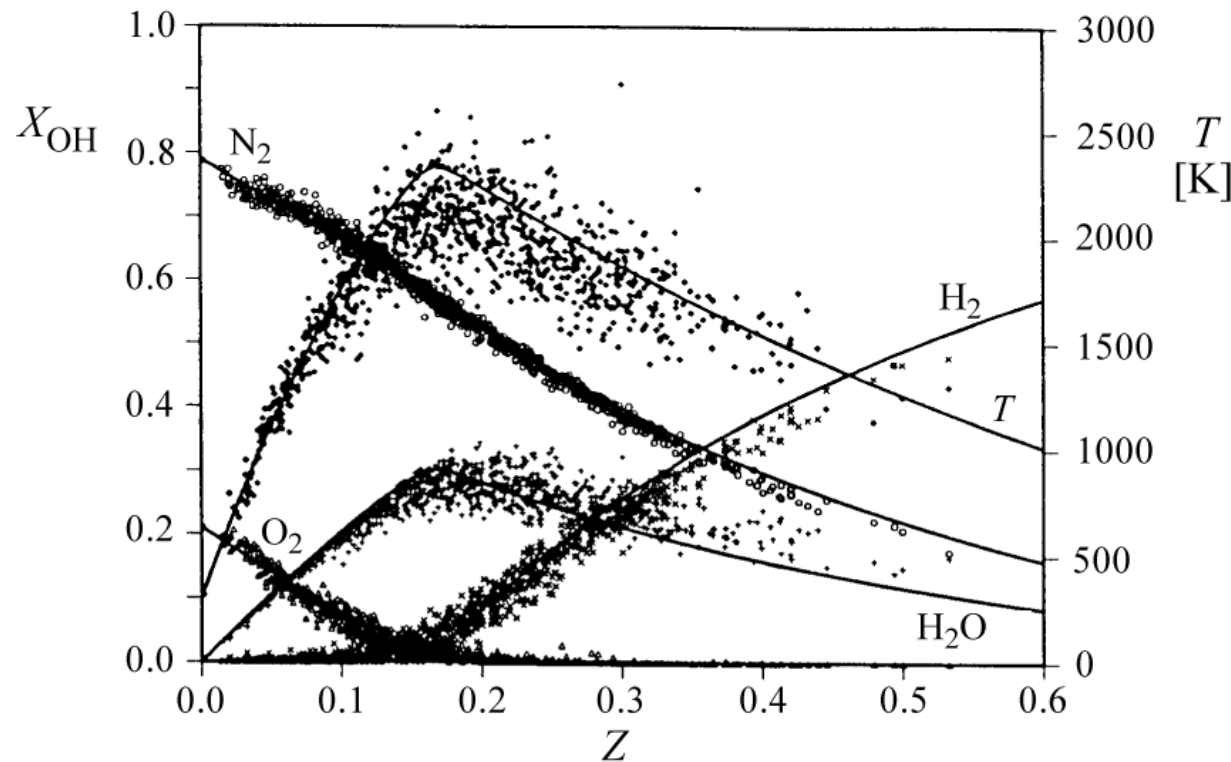
- 1) a fully turbulent part,
- 2) an outer flow part and
- 3) a part which was related to the viscous superlayer between the outer flow and the fully turbulent flow region.

The model shows that the intermediate maximum is due to the contribution from the fully turbulent part of the scalar field.

The overall agreement between the experimental data and the equilibrium solution is quite good.

This is often observed for hydrogen flames where chemistry is typically very fast.

On the contrary,
hydrocarbon flames
at high exit velocities and
small nozzle diameters are
likely to exhibit local
extinction and
non-equilibrium effects,
discussed in
Masri et al. (1996).



The equation

$$\rho \frac{\partial \psi_i}{\partial t} = \frac{\rho}{Le_i} \frac{\chi}{2} \frac{\partial \psi_i}{\partial Z} + \omega_i$$

shows that ψ_i depends on the mixture fraction Z , on the scalar dissipation rate χ , and on time t .

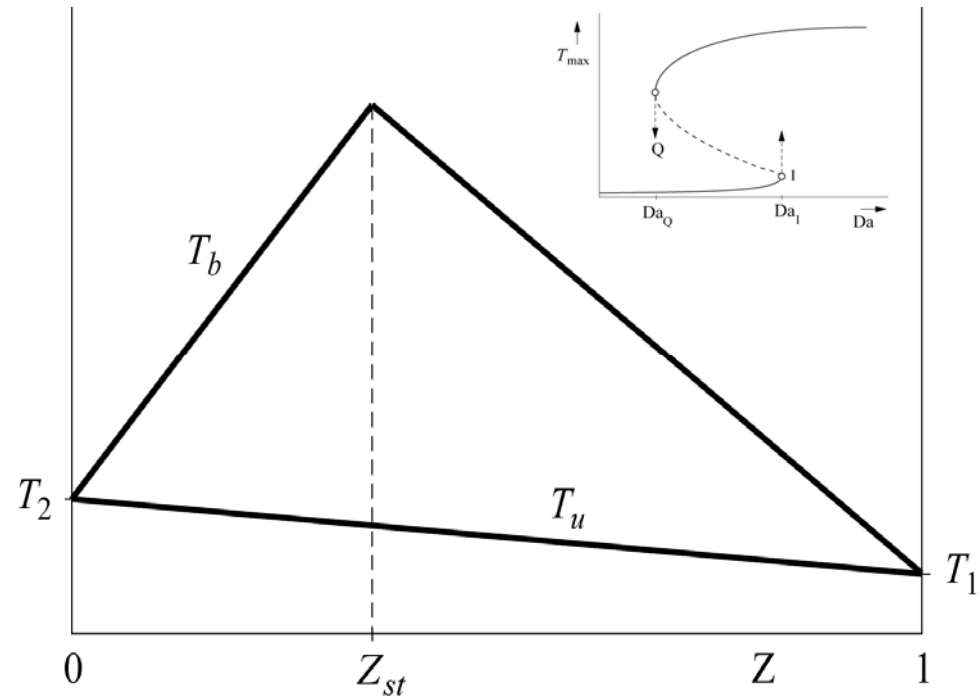
This implies that the reactive scalars are constant along iso-mixture fraction surfaces at a given time and a prescribed functional form of the scalar dissipation rate.

Thereby the fields of the reactive scalars are aligned to that of the mixture fraction and are transported together with it by the flow field.

Flamelet equations can also be used to describe ignition in a nonpremixed system.

If fuel and oxidizer are initially at the unburnt temperature $T_u(Z)$, as shown in the figure, but the scalar dissipation rate is still large enough, so that heat loss out of the reaction zone exceeds the Heat release by chemical reactions, a thermal runaway is not possible.

This corresponds to the steady state lower branch in the S-shaped curve.

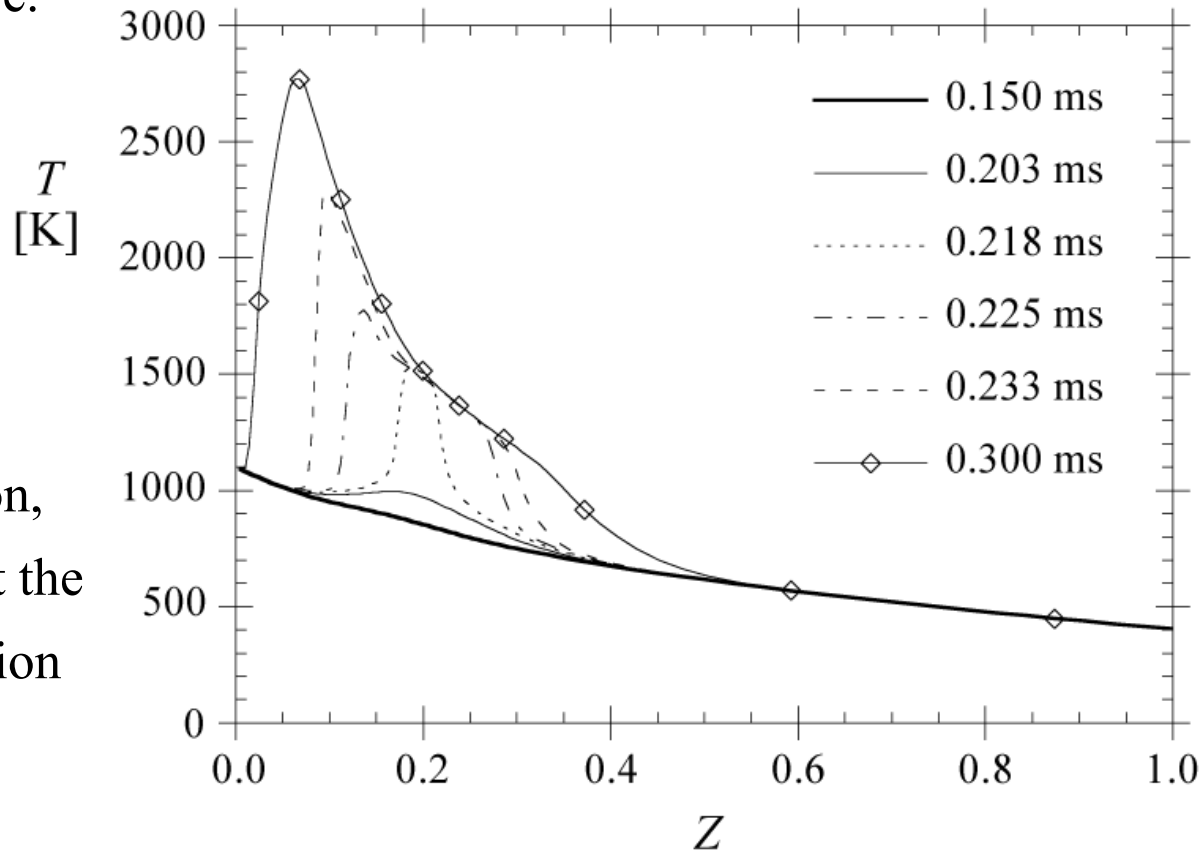


From thereon, the temperature profile broadens, which may be interpreted as a propagation of two fronts in mixture fraction space, one towards the lean and the other towards the rich mixture.

Although the transport term
in

$$\rho \frac{\partial \psi_i}{\partial t} = \frac{\rho}{Le_i} \chi \frac{\partial \psi_i}{\partial Z} + \omega_i$$

contributes to this propagation, it should be kept in mind that the mixture is close to auto-ignition everywhere.

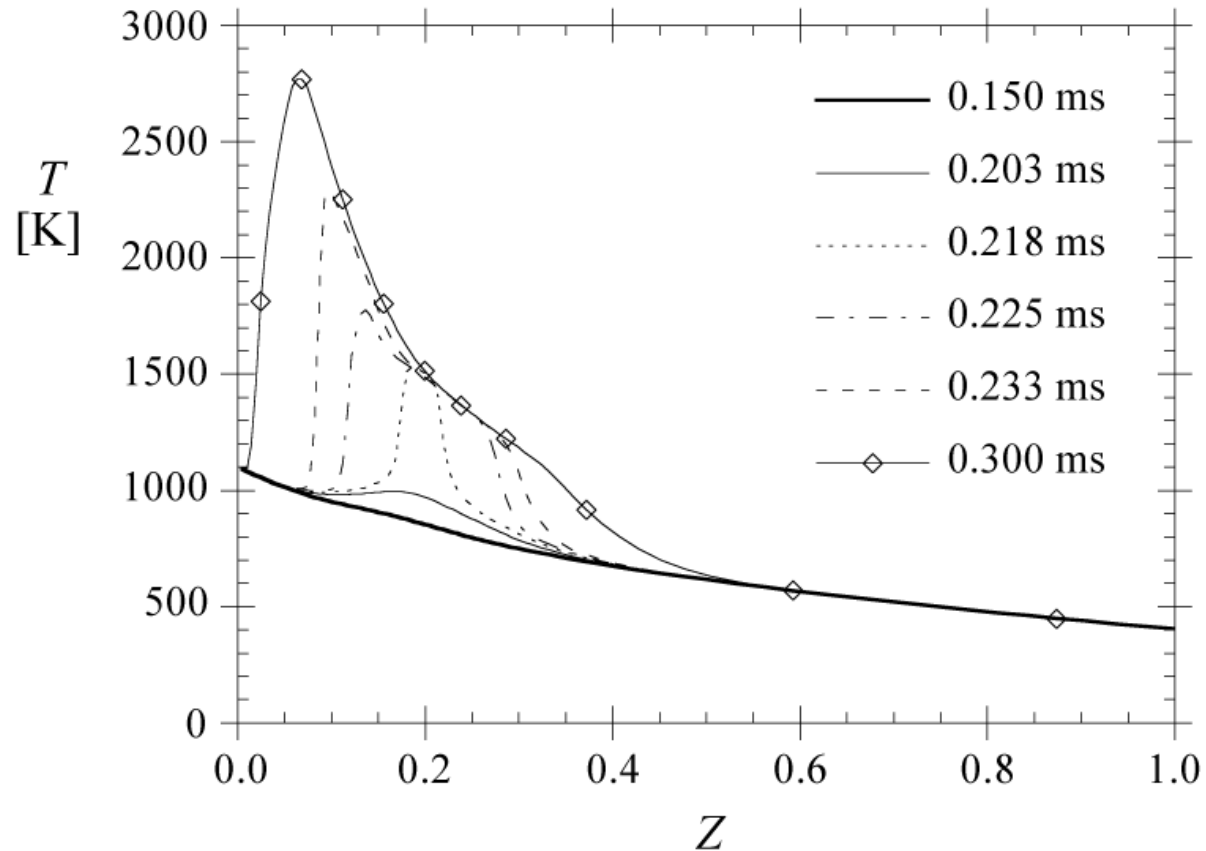


The propagation of an ignition front in mixture fraction space therefore differs considerably from premixed flame propagation.

At $t = 0.3$ ms most of the mixture, except for a region beyond $Z = 0.4$ in mixture fraction space, has reached the equilibrium temperature.

A maximum value of $T = 2750$ K is found close to stoichiometric mixture.

The ignition of n -heptane mixtures under Diesel engine condition has been discussed in detail by Pitsch and Peters (1998).



There it is shown that auto-ignition under nonpremixed conditions occurs mainly at locations in a turbulent flow field where the scalar dissipation rate is low.

It is interesting to note that by taking the values $S_{\text{NO}}(Z_b)=10.8 \cdot 10^{-3}/\text{s}$ and $\varepsilon=0.109$ for propane from Peters and Donnerhack (1981) and using

$$\left(\frac{3}{4}\beta \text{Fr}^* - \frac{1}{8}\right) \left(\frac{\beta L}{d_{\text{eff}}}\right)^2 + \left(\frac{\beta L}{d_{\text{eff}}}\right)^5 = \frac{3\beta \alpha_1^2}{16 Z_{\text{st}}^2} \text{Fr}^*$$

in the buoyancy dominated limit one calculates a factor of 27.2 rather than 22 in

$$\frac{E_{\text{NO}_x}}{d/u_0} = 27.2 \text{Fr}^{3/5} \left[\frac{\text{gNO}_2}{\text{kg fuel s}} \right]$$

Since Peters and Donnerhack (1981) had assumed equilibrium combustion chemistry, the second derivative of the temperature in

$$\varepsilon = \left(\frac{-2RT_b^2}{Z_b^2 E_{\text{NO}}(d^2T/dZ^2)_{T_b}} \right)^{1/2}$$

was calculated from an equilibrium temperature profile.

Therefore ε was tabulated as a constant for each fuel

If the quantity $S_{\text{NO}}(Z_b)d/u_0$ is interpreted as a Damköhler number the rescaled emission index from

$$\text{EINO} \sim S_{\text{NO}}(Z_b)\varepsilon \left(\frac{L}{d}\right)^3 \frac{d}{u_0}$$

is

$$\frac{\text{EINO}}{(L/d)^3} \sim \varepsilon \text{Da}$$

proportional to that Damköhler number.

Sanders et al. (1997) have reexamined steady state flamelet modeling using the two variable presumed shape pdf model for the mixture fractions and, either the scalar dissipation rate or the strain rate as second variable.

Their study revealed that only the formulation using the scalar dissipation rate as the second variable was able to predict the $Da^{1/2}$ dependence of the data of Driscoll et al. (1992).

This is in agreement with results of Ferreira (1996).

In addition Sanders et al. (1997) examined whether there is a difference between using a lognormal pdf of χ_{st} with a variance of unity and a delta function pdf and found that both assumptions gave similar results.

Their predictions improved with increasing Damköhler number and their results also suggest that $Le_i = 1$ is the best choice for these hydrogen flames.

For a turbulent jet flame with a fuel mixture of 31 % methane and 69 % hydrogen Chen and Chang (1996) performed a detailed comparison between steady state flamelet and pdf modeling.

They found that radiative heat loss becomes increasingly important for NO predictions further downstream in the flame.

This is in agreement with the comparison of time scales by Pitsch et al. (1998) who found that radiation is too slow to be effective as far as the combustion reactions are concerned, but that it effects NO levels considerably.